Original Paper

Developmental Neuroscience

Dev Neurosci 2010;32:268–277
DOI: 10.1159/000319663

Received: February 19, 2010
Accepted after revision: July 23, 2010
Published online: October 30, 2010

The Role of *Tuba1a* in Adult Hippocampal Neurogenesis and the Formation of the Dentate Gyrus

David A. Keays[a] James Cleak[b] Guo-Jen Huang[b] Andrew Edwards[b]
Andreas Braun[a] Christoph D. Treiber[a] Ruth Pidsley[b] Jonathan Flint[b]

[a]Institute of Molecular Pathology, Vienna, Austria; [b]Wellcome Trust Centre for Human Genetics, University of Oxford, Oxford, UK

Key Words
Neurogenesis · *Tuba1a* · Lissencephaly · Hippocampus · Dentate gyrus · Migration

Abstract
The multitubulin hypothesis holds that each tubulin isotype serves a unique role with respect to microtubule function. Here we investigate the role of the α-tubulin subunit *Tuba1a* in adult hippocampal neurogenesis and the formation of the dentate gyrus. Employing birth date labelling and immunohistological markers, we show that mice harbouring an S140G mutation in *Tuba1a* present with normal neurogenic potential, but that this neurogenesis is often ectopic. Morphological analysis of the dentate gyrus in adulthood revealed a disorganised subgranular zone and a dispersed granule cell layer. We have shown that these anatomical abnormalities are due to defective migration of prospero-homeobox-1-positive neurons and T-box-brain-2-positive progenitors during development. Such migratory defects may also be responsible for the cytoarchitectural defects observed in the dentate gyrus of patients with mutations in *TUBA1A*.

Introduction

Microtubules are composed of α-tubulin and β-tubulin heterodimers and are known to play a vital role in numerous cellular processes including intracellular trafficking, migration and mitosis. In mammals there are at least 7 genes that encode α-tubulins and another 7 for β-tubulins [Villasante et al., 1986; Oakley, 2000; Khodiyar et al., 2007]. While there is a high degree of homology within these two gene families, each tubulin isotype possesses a unique amino acid sequence with varying expression patterns [Sullivan et al., 1985, 1986; Khodiyar et al., 2007]. These differences have led to the multitubulin hypothesis, which holds that each tubulin isotype serves a specific role with respect to microtubule function [Fulton and Simpson, 1976; McKean et al., 2001]. Evidence in support of this proposition is limited because the raising of specific antibodies to study the different tubulin isotypes has proved difficult [Linhartová et al., 1992].

An alternative approach is to employ genetic tools, whereby the function of tubulins is investigated by studying the phenotypic consequences of mutating each tubulin isotype. For example, the generation of *Tubb1* knockout mice has revealed that this particular tubulin isotype plays an important role in the synthesis, structure and

KARGER

Fax +41 61 306 12 34
E-Mail karger@karger.ch
www.karger.com

0378–5866/10/0324–0268$26.00/0

Accessible online at:
www.karger.com/dne

David A. Keays
Institute of Molecular Pathology
Dr. Bohr-Gasse 7
AT–1030 Vienna (Austria)
Tel. +43 1 797 303 530, Fax +43 1 798 7153, E-Mail keays@imp.ac.at

function of blood platelets [Schwer et al., 2001]. We have recently reported the identification of a dominant S140G mutation in *Tuba1a* in the *Jenna* mouse *(Jna/+)* [Keays et al., 2007]. The mutation impairs the ability of TUBA1A to bind guanosine triphosphate and results in a dramatic reduction in the efficiency of tubulin heterodimer formation. Consequently, neuronal migration is impaired, which results in a fractured pyramidal cell layer in the hippocampus and subtle layering defects in the cortex. The discovery that this gene is also mutated in humans suffering from lissencephaly further demonstrates the importance of TUBA1A for the migration of neurons [Poirier et al., 2007]. Its role, however, in mitotic division has not been explored.

Mitosis is a cellular process that is heavily dependent on microtubules. First, microtubules attach to kinetochores during prometaphase; then, in metaphase, they form the mitotic spindle facilitating the alignment of the sister chromatids, before mediating their separation in anaphase [Gadde and Heald, 2004]. Studies in the fly *Drosophila melanogaster* have shown that mutations in an α-tubulin subunit (αTUB67C) compromise meiotic and mitotic division [Matthews et al., 1993]. Similarly, in the fungus *Aspergillus nidulans,* mutations in both α-tubulins have been shown to disrupt mitosis by affecting the stability of the mitotic spindle [Morris, 1975; Gambino et al., 1984]. In this paper, we ask whether *Tuba1a* is required for cell division in the adult nervous system in mice.

We focused on the adult because *Tuba1a* expression is largely absent from the proliferative ventricular zones during development. In adulthood *Tuba1a,* in addition to being expressed in a wide array of neuronal structures [Bamji and Miller, 1996], is also expressed in the olfactory bulb, the rostral migratory stream and the subgranular zone (SGZ) of the dentate gyrus [Gloster et al., 1994; Coksaygan et al., 2006]. The generation of new neurons has been shown to persist in these regions postnatally [Altman and Das, 1966; Kaplan and Hinds, 1977], and in the case of the dentate gyrus progenitors located in the SGZ proliferate, migrate and differentiate becoming granule cells. These newly born neurons are thought to play an important role in a number of behaviours including spatial memory, fear conditioning and fear-related behaviours [Snyder et al., 2005; Saxe et al., 2006; Sahay and Hen, 2007]. A molecular defect in tubulin that affects the genesis of neurons could contribute to the abnormal spatial working memory and anxiety-based behaviour we observed in the *Jna*/+ mutant mice. Here we investigate this hypothesis.

Methods

Animals

Jna/+ mice and wild-type littermate male mice were maintained in a 12:12-hour light:dark cycle at a temperature of 22 ± 1°C with a humidity of 60–70%. Where possible, 5 mice were placed in each cage, and animals had access to food ad libitum. The genotype of the animals was determined by PCR analysis, as previously described [Keays et al., 2007], and only littermates were selected for experiments. *Tuba1a-LacZ* mice (K6) were obtained from the Miller group [Gloster et al., 1994], and the presence of the transgene was confirmed by amplifying and sequencing with the following primers: TUBA1A_LACZ_F1 GGGGGAGAGATTACCTCATA, and TUBA1A_LACZ_R1 TGCGCAACTGTTGGGAAG. All experiments were performed in accordance with the UK Animals (Scientific Procedures) Act 1986.

Bromodeoxyuridine Labelling

For our developmental studies, bromodeoxyuridine (BrdU) was injected intraperitoneally at embryonic day (E)14.5, brains from mutants and wild-type littermates were harvested at postnatal day (P)0 (n = 3), drop fixed in 4% paraformaldehyde and then sectioned on a cryostat. For pulse labelling experiments, male mice (n = 9) aged approximately 12 weeks were injected with BrdU (50 μg/g of body weight) on a single occasion, and perfused 24 h later with 0.9% NaCl, followed by 4% paraformaldehyde. For cell survival and differentiation experiments, 4 BrdU injections (50 μg/g of body weight) were administered over 4 consecutive days at approximately 12 weeks of age (n = 7), and the animals perfused 28 days later. The brains were removed, postfixed for 4–6 h and then dehydrated in 30% sucrose. Then, they were sectioned coronally (40 μm) on a sliding microtome (Leica) through the hippocampus and the sections stored at –20°C in antifreeze.

Permanent Staining

One in 8 sections was mounted on polylysine-coated slides (VWR Scientific) for immunostaining. Citrate buffer (0.01 M) antigen retrieval was performed, as previously described [Huang and Herbert, 2005]. For BrdU staining, the sections were then digested in trypsin (0.0125%) for 7 min at 37°C, washed 3 times in PBS, followed by a 30-min incubation in 2 N HCl at 37°C. Then they were incubated with the primary antibody overnight in 0.5% PBS/Triton with 2% sera at the following concentrations: BrdU (Accurate Chemical and Scientific; 1:100); doublecortin (DCX, 1:100; Santa Cruz) or Ki-67 (Vector; 1:3,000). The next day, following several washes in PBS, biotinylated secondary antibodies were applied for 2 h in 0.5% Triton with 2% serum for 2 h (Vector; 1:200). Staining was visualised by an avidin-biotin peroxidase system (Vectastain ABC kit; Vector Laboratories) and diaminobenzidine (Sigma).

Fluorescent Staining

Fluorescent staining was performed on either 30- or 40-μm floating sections. The sections were incubated with the primary antibody overnight in 0.3% Triton/PBS with 2% of the appropriate serum at the following concentrations: NeuroD (Chemicon; 1:100), prospero homeobox 1 (PROX1; Chemicon; 1:400), glial fibrillary acidic protein (GFAP; Dako; 1:500), DCX (Santa Cruz; 1:400), T-box brain 2 (TBR2; Abcam; 1:500), LACZ (Abcam;

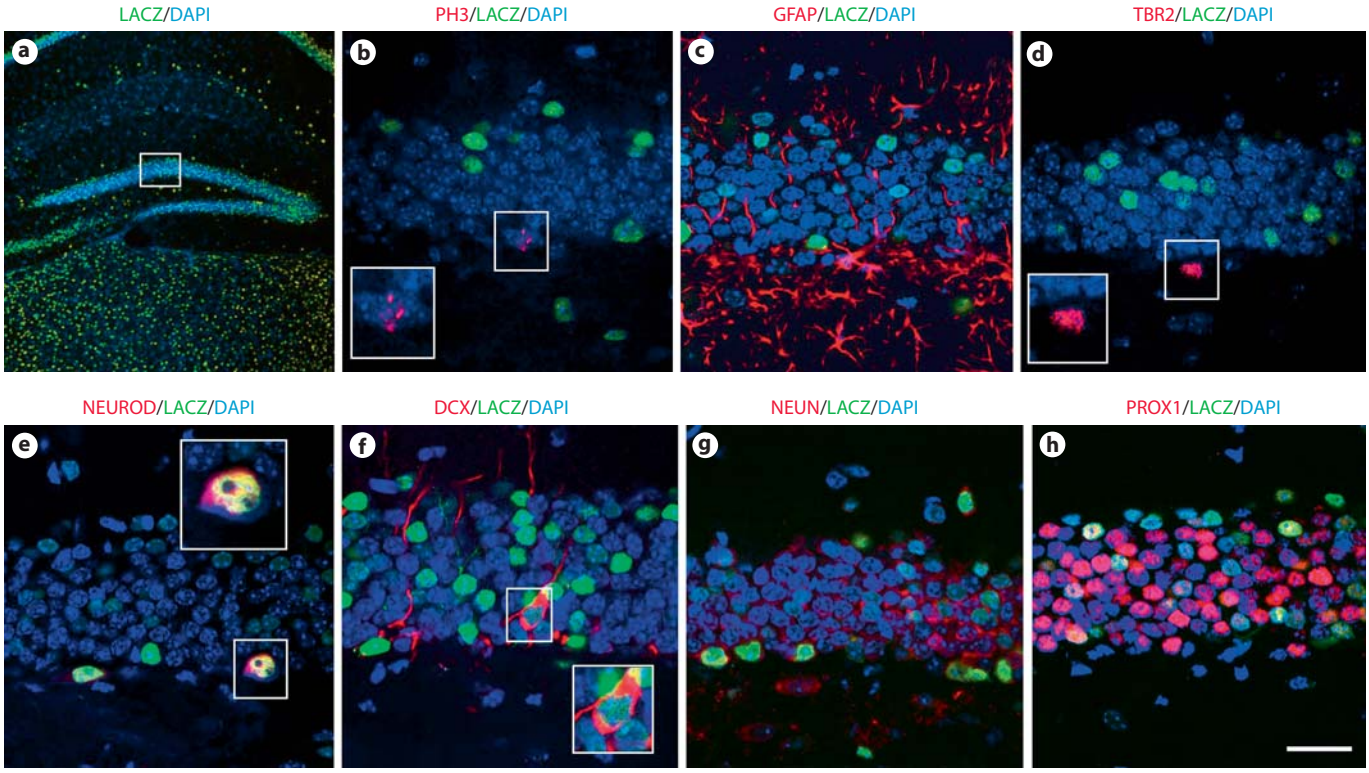

Fig. 1. Expression of Tuba1a-LacZ in the adult dentate gyrus. Blue: DAPI-stained nuclei. Scale bar = 20 μm. **a** Overview of the adult dentate gyrus in the coronal plane. LacZ expression (green) driven by a rodent *Tuba1a* promoter. **b–d** Staining with PH3 (**b**, red), GFAP (**c**, red) and TBR2 (**d**, red) revealed an absence of colocalisation with LacZ, indicating that *Tuba1a* is not expressed in neurogenic type 1 radial glial-like progenitors or type 2 intermediate progenitors. **e**, **f** NeuroD (**e**, red) and DCX staining (**f**, red) shows colocalisation with LacZ in the SGZ. **g**, **h** NeuN (**g**) and PROX1 (**h**) confirm the expression of *Tuba1a* in postmitotic neurons in the GCL.

1:1,000) and phosphohistone H3 (PH3; Chemicon; 1:200). For BrdU/NeuN double labelling, the sections were first incubated in 2 N HCl for 30 min at 37°C, neutralised in boric acid for 15 min (pH 8.5) and washed 3 times in PBS before incubation with antibodies for BrdU (Accurate Chemical and Scientific; 1:200) and NeuN (Chemicon; 1:400). Following 3 washes in PBS (5 min each), the sections were incubated with the appropriate fluorescent secondary antibody for 2 h at a concentration of 1:200 in 0.3% Triton/PBS with 2% sera.

Quantification

Images of one side of the dentate gyrus were captured on a TE2000 inverted microscope (Nikon) and then analysed using ImageJ (NIH). The total number of cells and the number of ectopic cells were counted in each section spaced 320 μm apart. A cell was deemed to be ectopic if it was observed within the granule cell layer (GCL). Total cell counts were determined by multiplying by 8 (for each section) and then doubled to account for both hemispheres. All cell counting was performed by J.C., who was blind to the genotype of the animals. For cell survival and differentiation studies, images were captured on a Zeiss LSM 510 confocal microscope, and a total of 30 BrdU-positive cells were analysed for coexpression with NeuN for each animal. To determine whether differences between groups of animals were significant, one-way ANOVAs were performed. In circumstances where the data failed to meet the assumptions of normality and equality of variance, transformations were performed. For expression studies, at least 100 DCX or PROX1 cells were selected randomly and inspected for colocalisation with LACZ.

Results

Tuba1a *Expression in the Dentate Gyrus*

Neurons born in the SGZ of the dentate gyrus express specific markers as they mature from radial glial-like progenitors (type 1: GFAP, nestin, PAX6 positive), to intermediate progenitor cells (type 2: TBR2 positive), to neuronal committed intermediate progenitors (type 3: NeuroD, DCX positive) to immature granule cells (type 4: calretinin, NeuN positive) and finally to mature granule cells (type 5: PROX1, calbindin positive) [von Bohlen und Halbach, 2007]. To investigate which of these cell

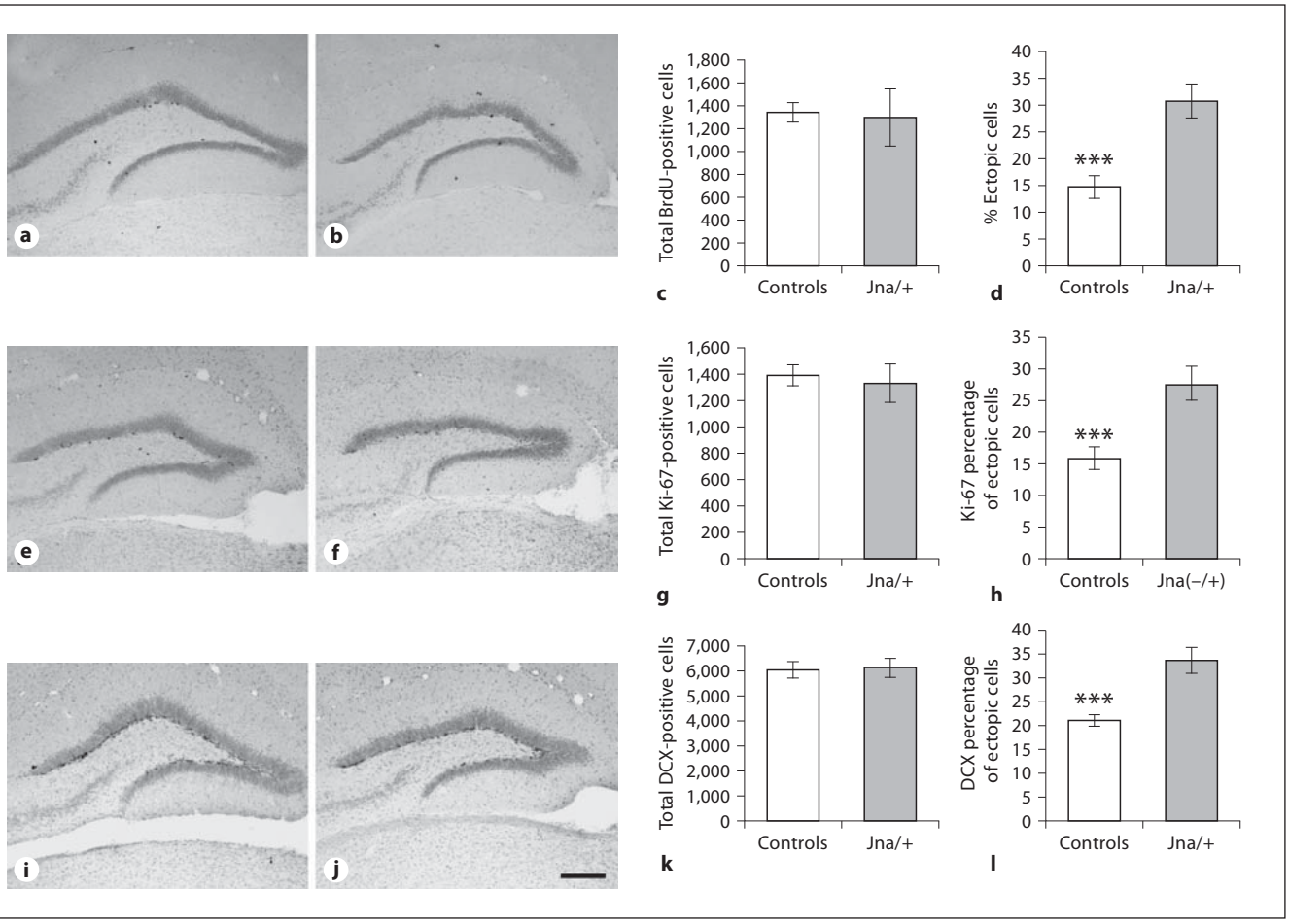

Fig. 2. Adult hippocampal neurogenesis in *Jna*/+ mutants. BrdU (**a**, **b**), Ki-67 (**e**, **f**) and DCX (**i**, **j**) staining on coronal sections of the dentate gyrus in *Jna*/+ mutants (**b**, **f**, **j**) and littermate controls (**a**, **e**, **i**). Blind counting of positive cells revealed no differences in neurogenic potential in affected animals when assessed by BrdU pulse labelling ($p > 0.1$), Ki-67 staining ($p > 0.5$) or DCX staining ($p > 0.5$; **c**, **g**, **k**). The number of ectopic neurons was significantly higher in *Jna*/+ mutants when staining with BrdU ($p < 0.005$), Ki-67 ($p < 0.0005$) and DCX ($p < 0.0005$; **d**, **h**, **l**). Scale bar = 100 μm.

types express *Tuba1a,* we utilised the *Tuba1a-LacZ* mouse line, which drives the expression of a *LacZ* transgene under the control of a rodent *Tuba1a* promoter. This mouse line has been widely used to define the expression pattern of *Tuba1a* and in general has been found to mirror the endogenous expression of *Tuba1a* mRNA [Gloster et al., 1994, 1999; Bamji and Miller, 1996]. Consistent with previous studies, we observed LACZ staining in the pyramidal cell layers of the hippocampus (CA1, CA2, CA3), and in the GCL of the dentate gyrus (fig. 1a). Within the dentate gyrus we did not observe clear colocalisation when staining with GFAP or TBR2 (n = 50), indicating that *Tuba1a* is not expressed in radial glial-like progenitors or intermediate progenitors (fig. 1c, d). We were able to detect clear colocalisation when staining with DCX and NeuroD, suggesting that *Tuba1a* is expressed in type 3 progenitors (fig. 1e, f). However, as DCX and NeuroD expression persists in young postmitotic neurons, we additionally stained with an antibody against PH3, a marker for cells in the mitotic phase (fig. 1b). We did not observe colocalisation of LacZ with PH3 (n = 40), evidence that LacZ-positive cells, while being DCX and NeuroD positive, are not mitotically active. As expected, LacZ staining was also observed in postmitotic neurons (NeuN positive, fig. 1g) and mature granule cells (PROX1 positive, fig. 1h). Cell counting revealed that 23% of DCX-positive cells expressed LacZ (n = 100) (although LacZ staining in these cells was generally less intense than in those LacZ-

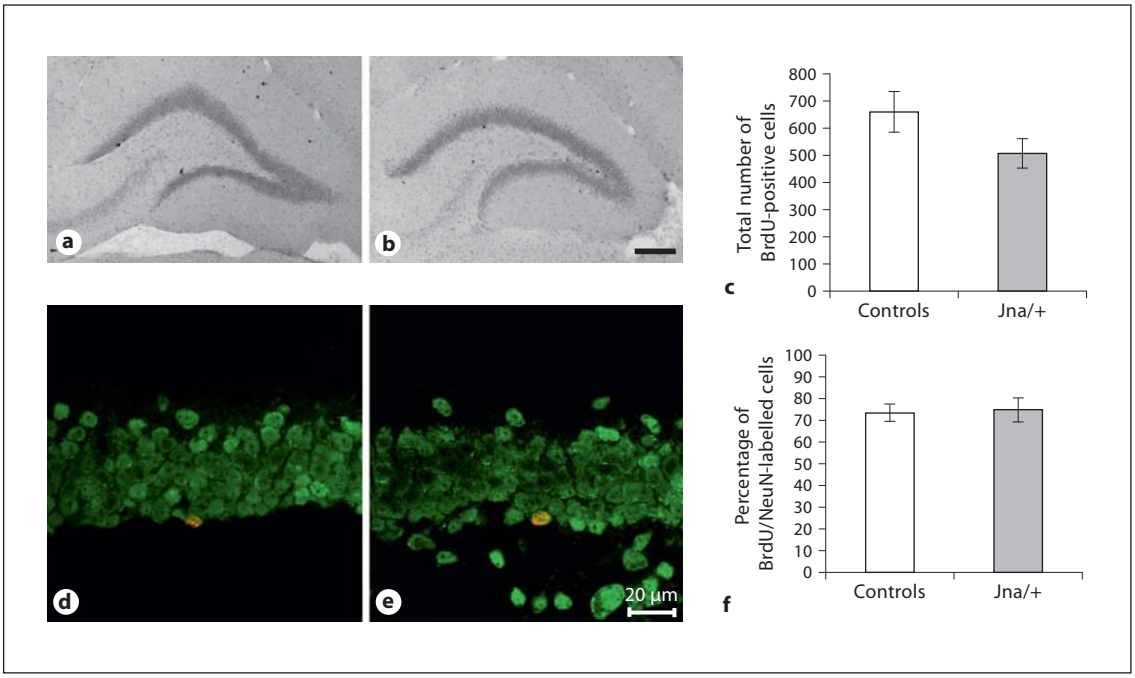

Fig. 3. Cell survival and differentiation in *Jna*/+ mutants. BrdU staining (**a–c**) on sections 28 days after 4 consecutive BrdU injections revealed a decrease in cell survival of newly born cells in the dentate gyrus of *Jna*/+ mutants; however, the reduction was not statistically significant ($p > 0.1$). Fluorescent double labelling on the same sections, employing BrdU and NeuN antibodies (**d–f**) revealed no significant difference in the percentage of double-labelled cells when comparing wild-type littermates (73%) and *Jna*/+ mutants (75%; $p > 0.5$) (**f**), which is indicative of normal neuronal differentiation. Scale bars = 100 μm (**a**, **b**) and 20 μm (**d**, **e**). **a**, **d** Controls. **b**, **e** *Jna*/+.

positive cells without DCX staining) and 25% of PROX1-positive cells expressed LacZ (n = 100).

Normal Neurogenesis, Differentiation and Cell Survival in Jna/+ *Mutants*

Given that *Tuba1a* in the adult hippocampus is limited in expression to postmitotic neurons, the S140G mutation in the *Jna*/+ mouse should not affect the neurogenic potential. To ascertain whether this is the case, we performed BrdU pulse labelling in male *Jna*/+ mutants and wild-type littermates (n = 9), and quantified BrdU-positive cells by cell counting blind to the genotype of the animals (fig. 2a–c). We observed no significant difference in the number of BrdU-labelled cells between mutants and controls [$F(1, 17) < 1$; $p > 0.1$]. A drawback of employing BrdU to assess neurogenesis is its reliance on an intraperitoneal injection, and its uncertain uptake by target cells [Wojtowicz and Kee, 2006]. We therefore confirmed this result by staining serial sections with Ki-67, a protein that is present during the active phases of the cell cycle and is indicative of mitotic activity [Yu et al., 1992] (fig. 2e–g). Again, we observed no difference between those animals harbouring the S140G mutation and wild-type littermates [$F(1, 17) < 1$; $p > 0.5$]. As BrdU and Ki-67 fail to distinguish between newly born glia and neurons, we also employed antibodies for DCX [Brown et al., 2003]. Staining with DCX, followed by cell counting, again showed no difference in neurogenesis in *Jna*/+ mutants, [$F(1, 19) < 1$; $p > 0.5$] (fig. 2i–k). The number of ectopic neurons, however, was significantly higher in *Jna*/+ mutants when staining with antibodies for BrdU [$F(1, 17) = 17.5$; $p < 0.001$], Ki-67 [$F(1, 19) = 17.9$; $p < 0.0005$] or DCX [$F(1, 19) = 28.5$; $p < 0.0005$] (fig. 2d, h, l). We then asked whether there was any difference in the ability of newly born cells to survive in *Jna*/+ mutants. To investigate this, we injected mutant and littermate controls with BrdU over 4 consecutive days, and sacrificed the animals 28 days later. Staining with a BrdU antibody revealed that there were fewer BrdU-positive cells in mutant animals, which is suggestive of increased cell death; however, this difference was not statistically significant [$F(1, 13) = 2.2$; $p > 0.1$) (fig. 3a–c). We also asked whether the S140G mu-

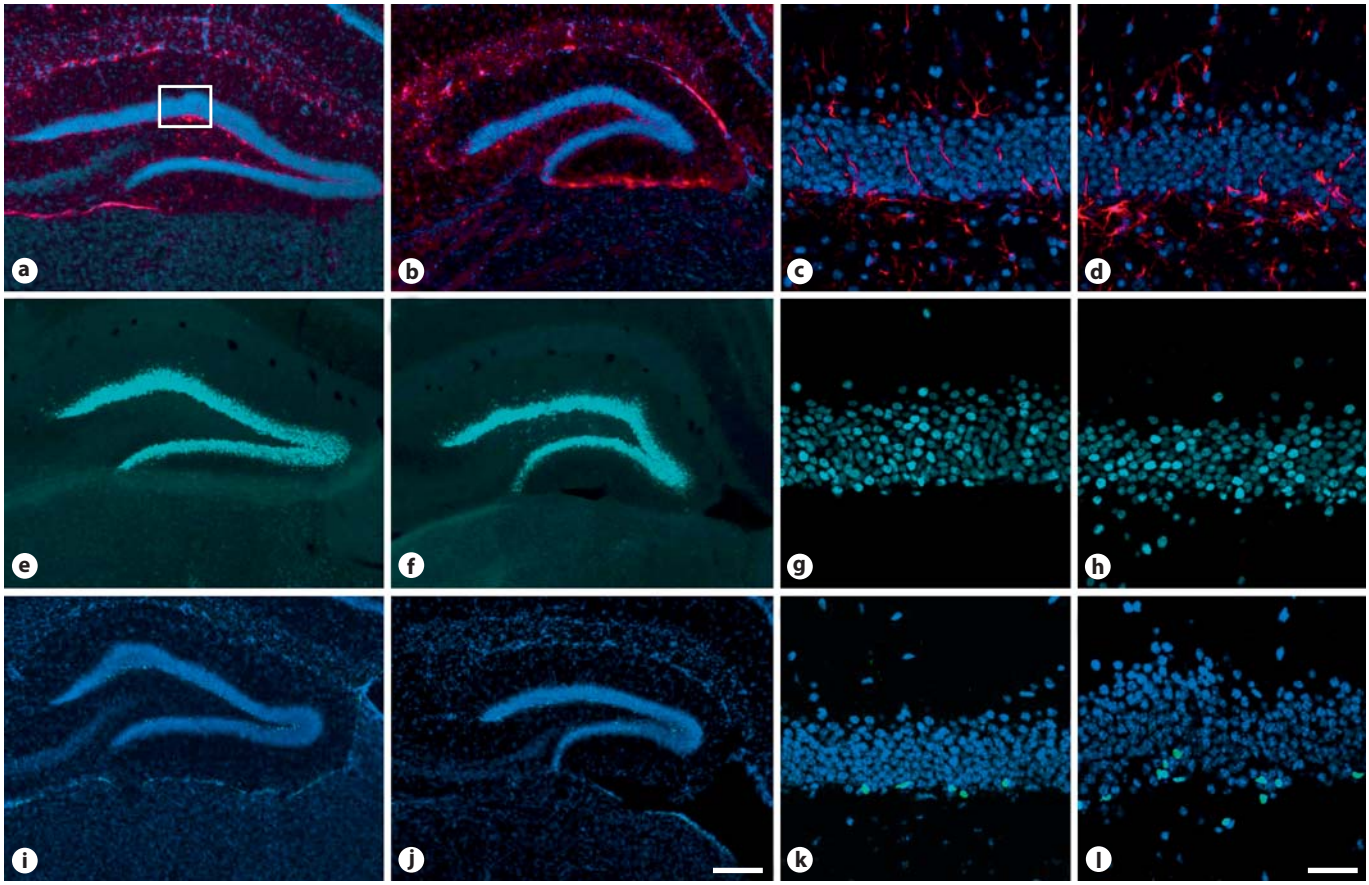

Fig. 4. Morphology of the adult dentate gyrus in *Jna*/+ mutants. Coronal sections of the dentate gyrus in *Jna*/+ mutants (**b**, **d**, **f**, **h**, **j**, **l**) and littermate controls (**a**, **c**, **e**, **g**, **i**, **k**) when stained with GFAP (**a–d**), PROX1 (**e–h**) and NeuroD (**i–l**). Staining with GFAP (red) showed a glial scaffold with cell bodies that are incorrectly localised to the GCL in *Jna*/+ mutants (**b**, **d**) when compared to wild-type littermates (**a**, **c**). NeuroD staining (green) revealed ectopic cells in *Jna*/+ mutants (**j**, **l**). NeuroD-positive cells could be observed within the GCL and in the hilus of the dentate gyrus. PROX1 (cyan), which labels mature granule cells, showed a dispersed GCL in *Jna*/+ mutants (**f**, **h**) in comparison to controls (**e**, **g**). DAPI staining (blue, **a–d**, **i–l**) confirms the presence of a dispersed GCL in affected animals. Scale bars = 100 μm (**j**) and 20 μm (**l**).

tation affects the ability of neurogenic precursors to differentiate into neurons. We employed double labelling, staining with sera for BrdU and NeuN (fig. 3d–f), and found that there was no significant difference in the percentage of NeuN-positive. BrdU-stained cells when comparing wild-type littermates (73%) and *Jna*/+ mutants [75%; $F(1, 13) < 1$; $p > 0.5$].

Disorganisation of the SGZ and GCL in Jna/+ *Mutants*

Our neurogenesis experiments showed that while the neurogenic potential in *Jna*/+ mutants is normal, ectopic neurogenesis is abundant. To investigate whether that is due to a disorganised SGZ, we stained adult *Jna*/+ mutants and littermate controls (n = 3) with GFAP to label radial glial progenitors (fig. 4a–d). In wild-type controls, GFAP-positive cell bodies were located in the SGZ, with fibres that extended perpendicularly into the GCL. In *Jna*/+ mutants the glial framework was present; however, some GFAP-positive cell bodies were located within the GCL, and the processes appeared less orthodox. To investigate this phenotype further, we employed sera to label NeuroD-positive cells that are normally located at the boundary of the GCL [von Bohlen und Halbach, 2007]. In *Jna*/+ mutants, NeuroD-positive cells were observed within the GCL and hilus of the dentate gyrus, confirming disorganisation of the SGZ (fig. 4i–l). Next we employed PROX1 staining to investigate the integrity of the

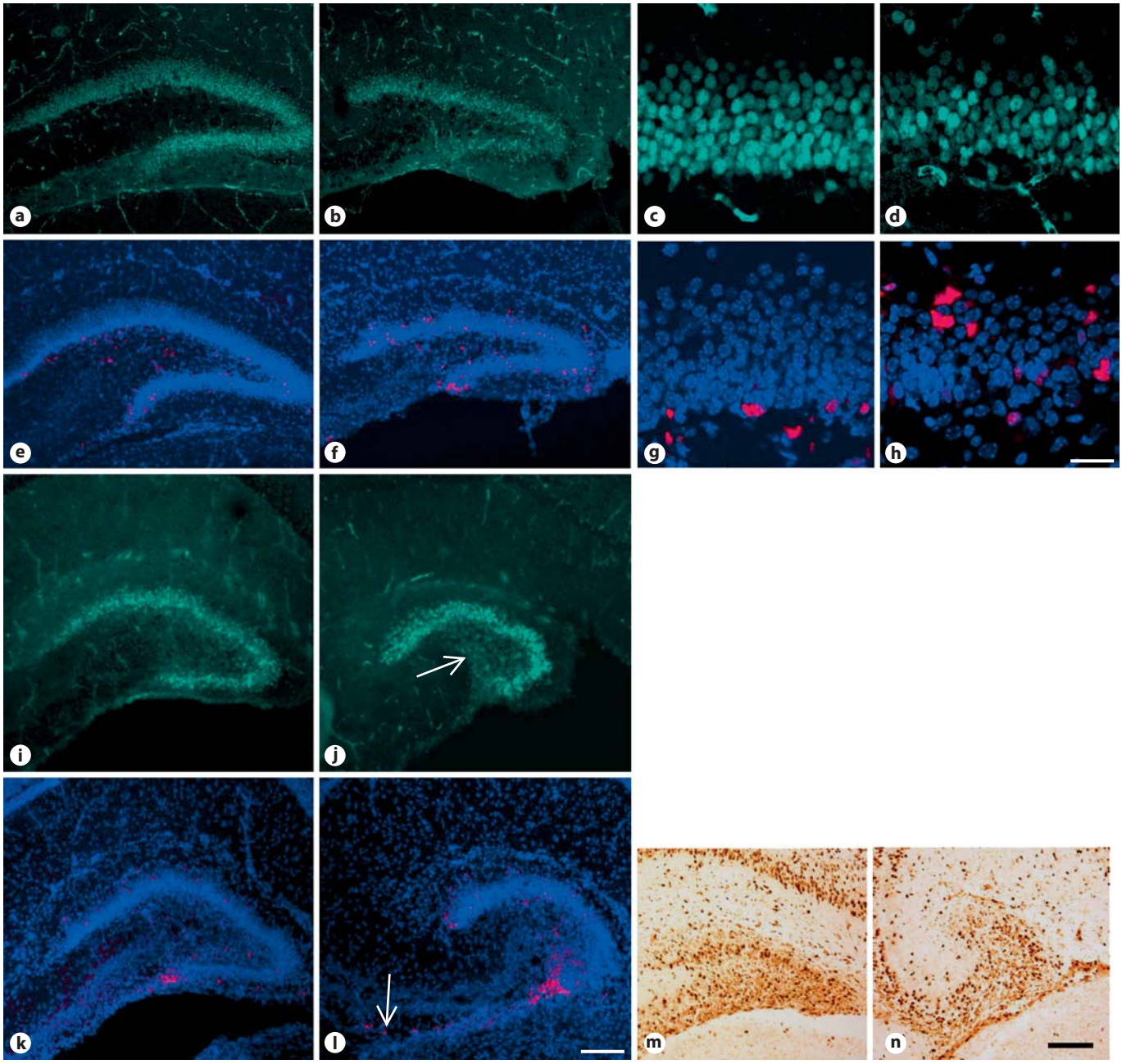

Fig. 5. The dentate gyrus of *Jna*/+ mutants during development. Coronal sections of the dentate gyrus in *Jna*/+ mutants (**b**, **d**, **f**, **h**, **j**, **l**) and littermate controls (**a**, **c**, **e**, **g**, **i**, **k**) when stained with PROX1 (**a–d**, **i**, **j**) and TBR2 (**e–h**, **k**, **l**) at P10 (**a–h**) and P4 (**i–l**). The panels on the right (**c**, **d**, **g**, **h**) show high-magnification images of the GCL in panels **a**, **b**, **e** and **f**. PROX1-positive granule cells are dispersed in *Jna*/+ mutants at P10 (**b**), and more severely at P4 (**j**). There is a notable presence of PROX1-positive cells in the hilus of mutant animals at P4 (**j**, arrow). TBR2 staining at P10 (**e–h**) shows positively stained cells scattered throughout the GCL, and in the molecular cell layer in *Jna*/+ mutants (**f**, **h**). At P4, a trail of TBR2-positive cells (**l**, arrow) is observed along the subpial stream, suggesting a defect in migration in *Jna*/+ mutants. BrdU labelling at E14.5, followed by sacrificing at P0 (**m**, **n**), confirms a migration phenotype. In *Jna*/+ mutants (**n**), BrdU-positive cells form a concave cluster in comparison to the clearly discernable suprapyramidal blade in wild-type controls (**m**). Scale bars = 100 μm (**l**, **n**) and 20 μm (**h**).

GCL [Elliott et al., 2001]. This revealed dispersion of granule cells in *Jna*/+ mutants (n = 3), with neurons present in the hilus and molecular layer (fig. 4e–h).

The Disorganised SGZ and GCL Are due to a Defect in Migration during Development

To ascertain whether the observed granule cell dispersion and disorganisation of the SGZ was the result of abnormal developmental processes or defective neuronal migration during adulthood, we examined wild-type and *Jna*/+ mutants at P4 (n = 3) when the radial organisation of the dentate cell layer is accomplished, and then again at P10 (n = 3) when it is further condensed and the neurogenic SGZ is in place [Li and Pleasure, 2007]. At P10, PROX1 staining revealed granule cell dispersion in *Jna*/+ mutants which was more severe than in the adult phenotype, which was notably worse at P4 (fig. 5a–d). At P4, both the suprapyramidal and infrapyramidal blades of the dentate gyrus lack their characteristic structure with a large number of PROX1-positive cells present in the hilus (fig. 5i, j). TBR2 staining of intermediate progenitors revealed the origins of the disorganised SGZ in *Jna*/+ mutants. In mutant animals, TBR2-positive cells were scattered throughout the GCL and were visible in the molecular layer, whereas in control animals most TBR2-positive cells were predominantly found at the helm of the GCL or in the hilus (fig. 5e–h). At P4, we observed a cluster of TBR2-positive cells located at the tip of the infrapyramidal blade in both *Jna*/+ mutants and wild-type controls in addition to a loose scattering throughout the hilus, GCL and molecular layer. While little difference was observed between mutants and wild-type controls in this respect, there was a striking trail of TBR2-positive cells along the subpial route in *Jna*/+ mutants, indicative of a defect in migration (fig. 5k, l). To investigate this further, we undertook a birth date labelling study, injecting BrdU at E14.5 (a time when both TBR2-positive progenitor cells and dentate granular cells are proliferating in the dentate notch), and then sectioned and stained *Jna*/+ mutants and wild-type littermates at P0 with sera for BrdU. In wild-type animals a clearly defined suprapyramidal blade consisting of BrdU-positive cells was apparent, whereas in *Jna*/+ mutants we observed an underdeveloped concave cluster of BrdU-positive cells (fig. 5m, n). Taken together, these data point towards a defect in the migration of both TBR2- and PROX1-positive cells. The result is a disorganised GCL and SGZ of the dentate gyrus that progressively improves but is still apparent in adulthood.

Discussion

In this paper, we have investigated the expression pattern of *Tuba1a* in the dentate gyrus as well as the neurogenic potential and morphology of the dentate gyrus in mice with an S140G mutation in *Tuba1a*. Employing a *Tuba1a-LacZ* mouse, we have observed colocalisation of LacZ with NeuroD, DCX, NeuN and PROX1, but not with GFAP, TBR2 or PH3. This result indicates that *Tuba1a* is expressed in early born postmitotic neurons (type 4) and mature granule cells (type 5), but not in radial glial-like (type 1) or intermediate progenitors (types 2 and 3) undergoing cellular division. It is not clear why only a percentage of DCX-, NeuN- and PROX1-positive cells stained positive for LacZ, given that *Tuba1a* is generally considered to be panneuronal. One explanation could be that partial penetrance plays a role, which may be a result of the genomic insertion site of the transgene [Bamji and Miller, 1996].

Consistent with the absence of *Tuba1a* in mitotically active progenitors, we have shown that *Jna*/+ mutant mice exhibit similar levels of adult neurogenesis to wild-type mice when assessed by three different means (BrdU, DCX, Ki-67), with no significant differences in the ability of new neurons to differentiate. Newly born neurons are, however, more likely to be ectopic, which is a consequence of a disorganised SGZ that is accompanied by granule cell dispersion. These findings are similar to those described in the *Lis1(+/–)* mutant mouse, which models another form of dominant lissencephaly. Like the *Jna*/+ mouse, the *Lis1(+/–)* mouse exhibits no defects in the genesis of neurons in the adult hippocampus, and presents with granule cell dispersion in the dentate gyrus with evidence of ectopic neurogenesis [Wang and Baraban, 2007]. Granule cell dispersion has also been reported in the reeler mutant mouse [Drakew et al., 2002; Zhao et al., 2004], and it has been shown that *Reelin* is required for the correct formation of the radial glial scaffold, for the migration of PROX1-positive granule cells, and for the transition of neurogenic precursors from the subpial zone to SGZ [Frotscher et al., 2003; Li et al., 2009].

Like the reeler mouse, the disorganisation of the dentate gyrus in the *Jna*/+ mouse has its origins in development. In the *Jna*/+ mouse, we observed granule cell dispersion at P10, and mislocalisation of PROX1-positive cells in the hilus at P4. In addition, TBR2-positive progenitors still line the subpial route at P4, and TBR2-positive cells are scattered throughout the GCL at P10. These observations suggest a defect in the migration of both these cellular populations. Neurogenic precursors (both

nestin and TBR2 positive) as well as the first granule cell neurons begin their migration from a region of the dorsomedial part of the telencephalic vesicles, known as the dentate notch, at around E13.5–14.5 [Li and Pleasure, 2007]. These cells migrate along the subpial stream before nestin-positive progenitors fan out and occupy the hilus (E17.5), the granule cells start forming the suprapyramidal blade (E18.5) and the TBR2-positive progenitors form the neurogenic subpial zone (E18.5). In due course, PROX1-positive granule cells are generated within the hilus, forming the infrapyramidal blade, and the TBR2-positive cells migrate through the molecular cell layer, settling in the SGZ alongside the nestin-positive progenitors [Li et al., 2009]. In the case of the *Jna*/+ mice our results indicate that, in addition to defective migration of postmitotic PROX1-positive granule cells, both the ventricular-to-subpial and subpial-to-subgranular migration of TBR2-positive cells is impaired. Such migratory defects may also be responsible for the unusual cytoarchitecture of the dentate gyrus reported in humans with mutations in *TUBA1A* [Fallet-Bianco et al., 2008]. For instance, a 24-week-old fetus carrying an I238V mutation in TUBA1A has an abnormally shaped dentate gyrus, lacking a compact defined GCL. Similarly, a 22-week-old fetus carrying a P263T mutation in TUBA1A was found to have an undeveloped hippocampus, a near absence of granule cells and little evidence that the dentate gyrus had started to form [Fallet-Bianco et al., 2008].

In summary, our results indicate that *Tuba1a* is vital for the proper formation of the dentate gyrus, but that it is not essential for adult hippocampal neurogenesis. This result suggests that another of the six α-tubulins is responsible for generating the tubulin heterodimers necessary for spindle formation and mitotic division in neurogenic progenitors. The identification and characterisation of this tubulin isoform will be of interest.

Acknowledgement

We wish to express our sincere thanks to Dr. Freda Miller for giving us the *Tuba1a-LacZ* mouse line.

References

Altman J, Das GD (1966): Autoradiographic and histological studies of postnatal neurogenesis. 1. A longitudinal investigation of the kinetics, migration and transformation of cells incorporating tritiated thymidine in neonate rats, with special reference to postnatal neurogenesis in some brain regions. J Comp Neurol 126:337–389.

Bamji SX, Miller FD (1996): Comparison of the expression of a Tα1:nlacZ transgene and Tα1 α-tubulin mRNA in the mature central nervous system. J Comp Neurol 374:52–69.

Brown JP, Couillard-Després S, Cooper-Kuhn CM, et al (2003): Transient expression of doublecortin during adult neurogenesis. J Comp Neurol 467:1–10.

Coksaygan T, Magnus T, Cai J, et al (2006): Neurogenesis in Tα-1 tubulin transgenic mice during development and after injury. Exp Neurol 197:475–485.

Drakew A, Deller T, Heimrich B, et al (2002): Dentate granule cells in reeler mutants and VLDLR and ApoER2 knockout mice. Exp Neurol 176:12–24.

Elliott RC, Khademi S, Pleasure SJ, et al (2001): Differential regulation of basic helix-loop-helix mRNAs in the dentate gyrus following status epilepticus. Neuroscience 106:79–88.

Fallet-Bianco C, Loeuillet L, Poirier K, et al (2008): Neuropathological phenotype of a distinct form of lissencephaly associated with mutations in TUBA1A. Brain 131(pt 9):2304–2320.

Frotscher M, Haas CA, Förster E (2003): Reelin controls granule cell migration in the dentate gyrus by acting on the radial glial scaffold. Cereb Cortex 13:634–640.

Fulton C, Simpson PA (1976): Selective synthesis and utilization of flagellar tubulin: the multi-tubulin hypothesis. Harbor Conf Cell Prolif 3:987–1005.

Gadde S, Heald R (2004): Mechanisms and molecules of the mitotic spindle. Curr Biol 14:R797–R805.

Gambino J, Bergen LG, Morris NR (1984): Effects of mitotic and tubulin mutations on microtubule architecture in actively growing protoplasts of *Aspergillus nidulans*. J Cell Biol 99:830–838.

Gloster A, El-Bizri H, Bamji SX, et al (1999): Early induction of Tα1 α-tubulin transcription in neurons of the developing nervous system. J Comp Neurol 405:45–60.

Gloster A, Wu W, Speelman A, et al (1994): The Tα1 α-tubulin promoter specifies gene expression as a function of neuronal growth and regeneration in transgenic mice. J Neurosci 14:7319–7330.

Huang GJ, Herbert J (2005): Serotonin modulates the suppressive effects of corticosterone on proliferating progenitor cells in the dentate gyrus of the hippocampus in the adult rat. Neuropsychopharmacology 30:231–241.

Kaplan MS, Hinds JW (1977): Neurogenesis in the adult rat: electron microscopic analysis of light radioautographs. Science 197:1092–1094.

Keays DA, Tian G, Poirier K, et al (2007): Mutations in α-tubulin cause abnormal neuronal migration in mice and lissencephaly in humans. Cell 128:45–57.

Khodiyar VK, Maltais LJ, Ruef BJ, et al (2007): A revised nomenclature for the human and rodent α-tubulin gene family. Genomics 90:285–289.

Li G, Kataoka H, Coughlin SR, et al (2009): Identification of a transient subpial neurogenic zone in the developing dentate gyrus and its regulation by Cxcl12 and reelin signaling. Development 136:327–335.

Li G, Pleasure SJ (2007): Genetic regulation of dentate gyrus morphogenesis. Prog Brain Res 163:143–152.

Linhartová I, Dráber P, Dráberová E, et al (1992): Immunological discrimination of β-tubulin isoforms in developing mouse brain: post-translational modification of non-class-III β-tubulins. Biochem J 288(pt 3):919–924.

Matthews KA, Rees D, Kaufman TC (1993): A functionally specialized α-tubulin is required for oocyte meiosis and cleavage mitoses in *Drosophila*. Development 117:977–991.

McKean PG, Vaughan S, Gull K (2001): The extended tubulin superfamily. J Cell Sci 114(pt 15):2723–2733.

Morris NR (1975): Mitotic mutants of *Aspergillus nidulans*. Genet Res 26:237–254.
Oakley BR (2000): An abundance of tubulins. Trends Cell Biol 10:537–542.
Poirier K, Keays DA, Francis F, et al (2007): Large spectrum of lissencephaly and pachygyria phenotypes resulting from de novo missense mutations in tubulin alpha 1A (TUBA1A). Hum Mutat 28:1055–1064.
Sahay A, Hen R (2007): Adult hippocampal neurogenesis in depression. Nat Neurosci 10: 1110–1115.
Saxe MD, Battaglia F, Wang JW, et al (2006): Ablation of hippocampal neurogenesis impairs contextual fear conditioning and synaptic plasticity in the dentate gyrus. Proc Natl Acad Sci USA 103:17501–17506.
Schwer HD, Lecine P, Tiwari S, et al (2001): A lineage-restricted and divergent β-tubulin isoform is essential for the biogenesis, structure and function of blood platelets. Curr Biol 11:579–586.
Snyder JS, Hong NS, McDonald RJ, et al (2005): A role for adult neurogenesis in spatial long-term memory. Neuroscience 130:843–852.
Sullivan KF, Havercroft JC, Machlin PS, et al (1986): Sequence and expression of the chicken beta 5- and beta 4-tubulin genes define a pair of divergent beta-tubulins with complementary patterns of expression. Mol Cell Biol 6:4409–4418.
Sullivan KF, Lau JT, Cleveland DW (1985): Apparent gene conversion between β-tubulin genes yields multiple regulatory pathways for a single β-tubulin polypeptide isotype. Mol Cell Biol 5:2454–2465.
Villasante A, Wang D, Dobner P, et al (1986): Six mouse α-tubulin mRNAs encode five distinct isotypes: testis-specific expression of two sister genes. Mol Cell Biol 6:2409–2419.
von Bohlen und Halbach O (2007): Immunohistological markers for staging neurogenesis in adult hippocampus. Cell Tissue Res 329: 409–420.
Wang Y, Baraban SC (2007): Granule cell dispersion and aberrant neurogenesis in the adult hippocampus of an LIS1 mutant mouse. Dev Neurosci 29:91–98.
Wojtowicz JM, Kee N (2006): BrdU assay for neurogenesis in rodents. Nat Protoc 1:1399–1405.
Yu CC, Woods AL, Levison DA (1992): The assessment of cellular proliferation by immunohistochemistry: a review of currently available methods and their applications. Histochem J 24:121–131.
Zhao S, Chai X, Förster E, et al (2004): Reelin is a positional signal for the lamination of dentate granule cells. Development 131:5117–5125.